

Simultaneous Quantification of Multiple Drugs by Machine Learning on Electrochemical Sensors

Tatsunori Matsumoto

Bio/CMOS Interfaces Laboratory (BCI)

École Polytechnique Fédérale de Lausanne / Shibaura Institute of Technology *École Polytechnique Fédérale de Lausanne*
Lausanne, Switzerland / Tokyo, Japan
tatsunori.matsumoto@epfl.ch / ma23177@shibaura-it.ac.jp

Lin Du

Bio/CMOS Interfaces Laboratory (BCI)

Lausanne, Switzerland

lin.du@epfl.ch

Yann Thoma

School of Engineering and Management Vaud

HES-SO University of Applied Sciences and Arts Western Switzerland

Yverdon-les-Bains, Switzerland

yann.thoma@heig-vd.ch

Sandro Carrara

Bio/CMOS Interfaces Laboratory (BCI)

École Polytechnique Fédérale de Lausanne

Lausanne, Switzerland

sandro.carrara@epfl.ch

Abstract—Electrochemical devices and systems are significant for the development of therapeutic drug monitoring (TDM) and personalized therapy. However, electrochemical sensors are usually not that much selective. Therefore, innovative machine learning (ML) approaches are now required to improve the selectivity at system level based on cyclic voltammograms (CV) obtained from electrochemical sensors in order to assure the quantification of several different drugs simultaneously present into the blood of patients. Based on an Artificial Neural Network (ANN), this paper proposes a novel model TwoWayANN along with an adaptive weighted cross-entropy loss (AWCEL) to address drugs interaction effectively and decline the quantification error range. The simulated dataset of etoposide (ETO) and methotrexate (MTX), proposed here as model drugs, is demonstrated to validate the efficacy of our proposed method. Our TwoWayANN model achieves the accuracy at 100% and 99.35% for ETO and MTX respectively within the error range of $\pm 5\mu\text{M}$. Our results are important for the development of point-of-care systems for applications in personalized therapy.

Index Terms—Therapeutic Drug Monitoring, Machine Learning, Cyclic Voltammogram, Multi-Drug Quantification, Personalized Therapy

I. INTRODUCTION

Chemotherapeutic therapy is extensively employed in cancer treatment, with oncology representing the primary domain for clinical research and the development of cancer therapies [1]. However, different anticancer drugs usually interact with each other, increasing side effects and toxicity. This can affect patient health and further increase the complexity of treatment planning and management [2]. Therefore, the development of point-of-care systems for therapeutic drug monitoring (TDM) in personalized dosage adjustment based on circulating drug concentrations in anticancer drugs is necessary [3], [4]. Multi-drug concentration quantification system presents significant advantages in the realm of cancer treatment. It facilitates the precise control of drug dosages through continuous monitoring of drug concentrations in the bloodstream, preventing potential toxicity due to overexposure and low treatment efficacy due

to underexposure [5]. The development of a new portable point-of-care device system for simultaneous quantification of multiple drug concentrations is essential to achieve this target.

Cyclic voltammograms (CV) obtained by electrochemical sensors and cyclic voltammetry techniques [6] can be a reliable tool to extract drug quantitative information and observe drugs interactions by analyzing variant redox peaks [7]. Etoposide (ETO) [8] and Methotrexate (MTX) [9] are widely used anti-cancer drugs in chemotherapeutic therapy. The CV results in [10] obtained by the two-drug solution on single electrochemical sensor show the redox peaks influenced by the oxidation of one single drug and the interaction between ETO and MTX. Specifically, at a fixed concentration of MTX, the redox peak values of MTX decrease with increasing concentrations of ETO. However, the redox peak values of ETO are not affected by MTX concentration. The complex mutual and reciprocal interaction of different drugs has to be solved when achieving simultaneous quantification of multiple drugs. Local intelligence based on machine learning (ML) implemented on system with powerful ability to solve nonlinear correlation will be an efficient way to achieve personalized therapy for multiple drugs with complicated interactions.

Several models based on different ML algorithms have been established for concentration quantification. Support vector classifier (SVC) with an RBF kernel has been used to compensate fouling phenomenon and achieve continuous concentration monitoring of propofol [11]. An Artificial Neural Network (ANN)-based model has been proposed to complete the simultaneous detection of caffeine and chlorogenic acid by extracting features from CV results with electrochemical sensors [12]. However, there is no clear ML-based model designed for taking the advantage of the interactions between multiple drugs for more precise quantification.

Therefore, this paper introduces an optimized model based on an ANN algorithm, denoted as TwoWayANN, capable of simultaneous quantification of multiple drugs. The proposed

model is constructed by two branches and one concatenation structure for the quantification of each single drug and effective utilization of the interaction mechanism. Simultaneously, an adaptive weighted Cross-Entropy loss (AWCEL) is exploited to adjust weights based on error for mitigating error range and enhance overall the quantification accuracy. Our proposed method is successfully validated by a simulated CV dataset of ETO and MTX with interaction constructed by a mathematical estimation.

II. METHODOLOGY

In this section we present our method for the simultaneous quantification of both ETO and MTX, and we detail data preparation and our model structure. The overview of the entire workflow is shown in Fig. 1. First, cyclic voltammetry acquisition is performed on a mixture of ETO and MTX solutions to obtain a CV result. As for the input of TwoWayANN model, the most distinct peaks associated with ETO and MTX are used instead of the entire CV series. After preprocessing, the single-peak current curves of ETO and MTX that appear in the acquired CV are inserted into the input layer of the TwoWayANN model as independent inputs, whose outputs are the type of drug and the concentration of each drug from the features learned in the model.

A. Preprocessing

The typical format of acquired CV data to be input here will be explained and shown in Fig. 2. Specifically, the CV data obtained from the mixture of ETO and MTX solutions has three peaks. The leftmost and center peak are peaks of ETO, and the rightmost peak is a peak of MTX. Here, we call the leftmost peak as first peak of ETO (Fig. 2 (a)) and the rightmost peak as last peak of MTX (Fig. 2 (b)), which are the most characteristic peaks of ETO and MTX. Then we extract each of first peak of ETO and last peak of MTX as separate input data and input them into TwoWayANN.

B. TwoWayANN Architecture

This section describes the TwoWayANN model architecture (Fig. 1) for quantifying the concentration of both ETO and MTX as classification tasks. The proposed TwoWayANN Architecture is based on the effective construction of classic and powerful ANN [13] blocks. When designing an ANN-based model for the quantification of individual concentrations of ETO and MTX, a distinct layer is required to extract the features of ETO and MTX respectively (Block-A), therefore a two-branch structure is constructed.

Subsequently, the features extracted from ETO and MTX are then concatenated to perform classifications regarding MTX concentrations as shown in Fig. 1. Given that concentrations of ETO are not affected by MTX, only the extracted features from ETO are utilized in the concentration classification process (Block-B). Block-C with more layers is constructed for MTX, which is influenced by ETO and occurring their chemical reactions, making the quantification task more complicated. It is important to emphasize that the

feature extraction process for ETO remains independent of MTX from input to output. Nevertheless, the feature extraction methodology for both substances follows a generally similar pattern. Each layer uses a linear function and an activation function ReLU to extract features. The linear function f and the ReLU function used for extracting features are as follows:

$$f(\mathbf{x}) = \mathbf{W}\mathbf{x} + \mathbf{b} \quad (1)$$

$$ReLU(f(\mathbf{x})) = (f(\mathbf{x}))^+ = \max(0, f(\mathbf{x})) \quad (2)$$

where \mathbf{x} is the extracted feature vector obtained from the outputs that go through each layer, \mathbf{W} and \mathbf{b} are the weight matrix and the bias vector respectively.

Ultimately, a multi-output submodule of TwoWayANN model is devised, where the quantified concentration of each drug is generated from the respective output layer for that drug, and solved as classification tasks. Loss function, an important part of this submodule, need to be improved based on typical Cross-Entropy loss [14], [15] which only accepts one output class. However, drug quantification tasks always have an allowable range, accepting multiple output classes with only minor drug-concentration differences.

C. Adaptive Weighted Cross-Entropy Loss

In order to mitigate the quantification error range of the output result from the aforementioned TwoWayANN model, an adaptive weighted Cross-Entropy loss (AWCEL) is proposed, i.e., the weights of the loss function are adaptive to quantification error. Firstly, the absolute error between the predicted label and the true label can be expressed as:

$$\mathbf{V}_{res} = |\arg\max(\tilde{\mathbf{y}}) - \mathbf{y}| \quad (3)$$

where $\tilde{\mathbf{y}}$ and \mathbf{y} are the predicted labels matrix and the true labels vector respectively. As $\arg\max(\tilde{\mathbf{y}})$ obtains the index of the maximum value in each row of the matrix $\tilde{\mathbf{y}}$, we can generate a vector with the same length as \mathbf{y} . Subsequently, by computing the difference between these two vectors, we can assess the extent deviating from the true labels. Ignoring the mathematic signs, the absolute values are calculated, and the aforementioned equation can be translated as follows:

$$\mathbf{V}_{res} = [v_1, v_2, \dots, v_n, \dots, v_N] \quad (4)$$

where N is a designated batch size. The values within residual vector \mathbf{V}_{res} serve as criteria for weight selection. Specifically, when a value v_n is smaller, it corresponds to a smaller difference from the true label. An increased weight should be assigned to the output value at that instance. Conversely, when the difference v_n is larger, the weight of the output is diminished intentionally to reduce its significance.

Here, the error range of the output concentration of the drug is set using a certain threshold th , which serves to determine the allowable margin of error for drug concentration quantification. According to the threshold th , the adaptive magnitude of the weights w_n can be represented as follows:

$$w_n = \begin{cases} (\log(th - v_n + 1))^{1/th} & (v_n < th) \\ 1/v_n * \log v_n & (v_n \geq th) \end{cases} \quad (5)$$

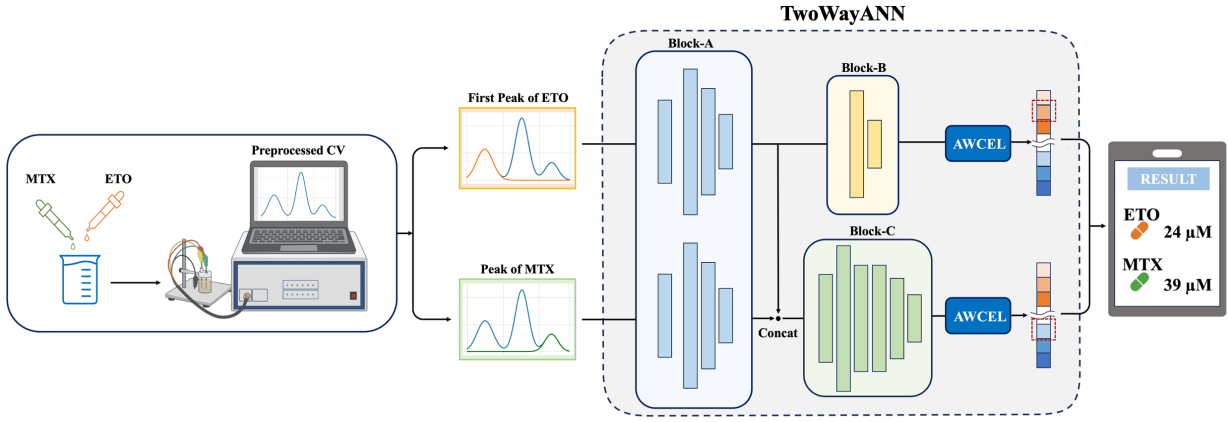


Fig. 1: Overall flowchart. The preprocessed CV results are obtained by electrochemical sensors and preprocessor. In TwoWayANN, we extract the features of the first peak of ETO and the peak of MTX by Block-A. In Block-B, features of linearity of ETO are extracted. Features of interaction between ETO and MTX are extracted by Block-C. The final drugs quantification is achieved by classification.

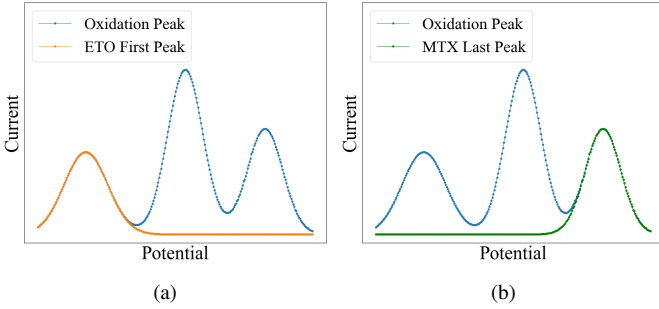


Fig. 2: CV example of (a) a first peak of ETO and (b) a last peak of MTX.

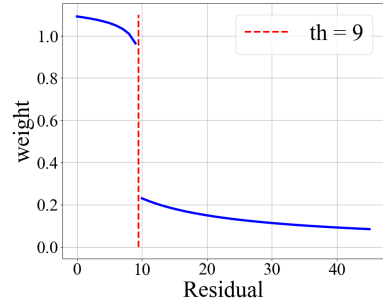


Fig. 3: An example of adaptive weight based on AWCEL.

The weights, computed for each error value within vector \mathbf{V}_{res} , are designed to exhibit significant disparities based on whether the error value exceeds or falls below the threshold th . As an example, the adaptive weights are shown in Fig. 3 when the threshold th is set to 9. The adaptive weight approximates 1 when the calculated error value (residual) is less than 9. However, when the error value exceeds 9, the weight diminishes to less than 0.2, signifying a reduction in importance. Applying the adaptive weight to the loss function is as follows:

$$AWCEL = - \sum_{n=1}^N \left[\log \frac{\exp(\max(\tilde{\mathbf{y}}_n))}{\sum_{c=1}^C \exp(\tilde{\mathbf{y}}_n^c)} \right] \cdot w_n \quad (6)$$

where C is the number of classes. By applying this weight to the Cross-Entropy loss, the weights can be adjusted prior to the backpropagation, leading to the reduction of the error range in the predicted drug concentration.

III. EXPERIMENTS

A. Data Preparation

A simulated dataset containing 10,000 samples was built based on the measured CV results shown in [10] and the

mathematical estimation demonstrated in [16], among which both the concentrations of ETO and MTX increase from $5 \mu\text{M}$ to $45 \mu\text{M}$ and each parameter has 10% fluctuation range to simulate the variation of experiment environment. The dataset is then split into a training, validation and test set of ratio 60%/20%/20%.

B. Results

Our proposed method is evaluated by the aforementioned simulated dataset, setting $1 \mu\text{M}$ as quantification resolution. In order to assess the performance of the TwoWayRNN architecture and proposed loss function AWCEL in the task of multi-drug quantification, the accuracy, Mean Absolute Percentage Error (MAPE), Mean Absolute Error (MAE), and Mean Squared Error (MSE) are introduced.

The Efficacy of the TwoWayANN Architecture. The quantification results of the TwoWayANN architecture without AWCEL is shown in Fig. 4. All of output values are concentrated around the true labels, i.e., the TwoWayANN can be an effective architecture to quantify the concentrations of ETO and MTX simultaneously. Specifically, the performance of quantifying ETO and MTX is shown in Table I (a). For ETO, the results of MAPE, MAE, and MSE are 4.064, 0.8938,

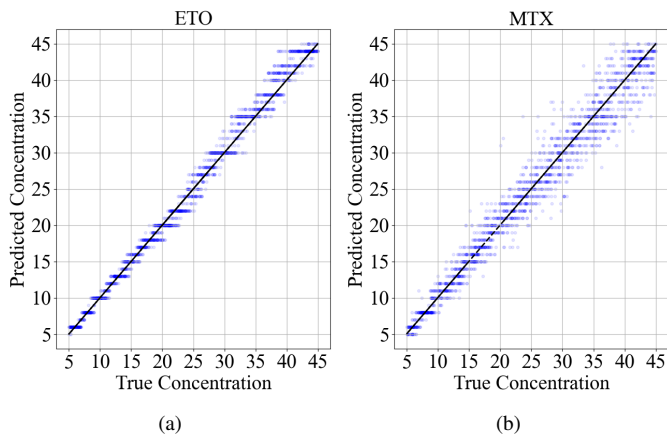


Fig. 4: Quantification Results of TwoWayANN without AWCEL. (a) The result of ETO. (b) The result of MTX.

and 1.335 respectively. For MTX, the results of MAPE, MAE, and MSE reach at 7.346, 1.653, and 5.306 respectively. Additionally, within the quantification error range of $\pm 5\mu M$, the accuracy shows 100% of ETO and 98.55% of MTX, indicating that a superb outcome has been achieved. However, within the error range of $\pm 1\mu M$, the accuracy of ETO and MTX are 95.70% and 79.90% respectively, showing a dramatical decrease of MTX. This result is due to the fact that the redox peak of MTX is affected by the ETO concentration, making the quantification of MTX more complicated. ETO, on the other hand, is not affected by MTX, so the quantification results of ETO can be maintained at a high level of accuracy.

TABLE I: Drugs Quantification Results Comparison

		Accuracy		MAPE	MAE	MSE
		$\pm 1\mu M$	$\pm 5\mu M$			
(a)	ETO	95.70%	100%	4.064	0.8938	1.335
	MTX	79.90%	98.55%	7.346	1.653	5.306
(b)	ETO	96.15%	100%	3.669	0.7851	0.9857
	MTX	86.05%	99.35%	5.487	1.292	3.136

(a) : TwoWayANN model without AWCEL
 (b) : TwoWayANN model equipped with AWCEL

The Efficacy of AWCEL. The results of TwoWayANN equipped with our proposed AWCEL are illustrated in Fig. 5 and demonstrate an improvement in the error range compared with Fig. 4. Specifically, the distortion and the variance in output values expressed in Fig. 5 is significantly mitigated and these output values are more concentrated around the true labels. Furthermore, the corresponding performance of the results of TwoWayANN equipped with AWCEL is also shown in Table I (b). For ETO, MAPE, MAE, and MSE reach at 3.669, 0.7851, and 0.9857 respectively. For MTX, the results of MAPE, MAE, and MSE are 5.487, 1.292, and 3.136 respectively. Equipped with AWCEL, all indicators obtain the best results and the error range has been reduced successfully. Additionally, within the quantification error range of $\pm 5\mu M$, the accuracy shows 100% of ETO and 99.35% of MTX. And the results of accuracy are 96.15% of ETO and 86.05% of

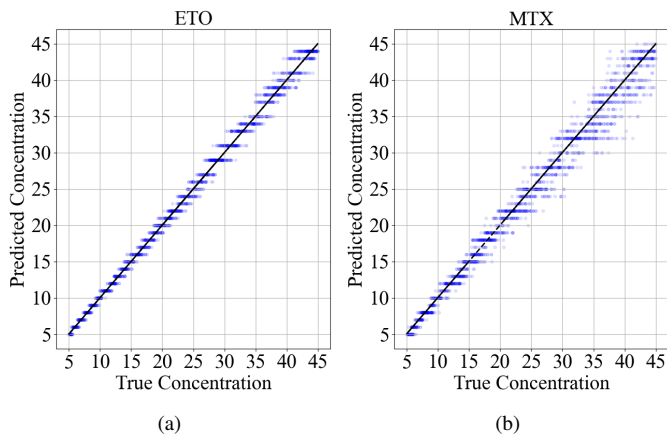


Fig. 5: Quantification Results of TwoWayANN equipped with AWCEL. (a) The result of ETO. (b) The result of MTX.

MTX within the error range of $\pm 1\mu M$. The previous problem of a dramatic decline in accuracy is restrained and the accuracy maintains over 86% of both drugs, proving the efficacy of adaptive weights of AWCEL.

Therefore, our proposed method combining TwoWayANN and AWCEL is validated for its efficacy in reducing the error range and improving the accuracy, capable of being an effective method for the simultaneous quantification of multiple drugs.

CONCLUSION

In this paper we demonstrated an effective ANN-based method to achieve simultaneous quantification of multiple drugs from data acquired through electrochemical sensors and cyclic voltammogram, offering new approaches for the development of personalized therapy systems for cancer treatments. The proposed TwoWayANN model with its specific structure designed for multiple drugs showing interaction mechanisms succeeded in quantifying the concentration of ETO and MTX with high accuracy. Additionally, we have also demonstrated that the use of AWCEL is able to optimize the typical Cross-Entropy loss using adaptive weights and further narrows down the quantification in a quite efficient and effective manner. The structure of our proposed method can be expanded for more complicated drugs quantification (e.g. interactions where both drugs have an impact on each other or more drugs). Furthermore, it presents great potential to integrate electrochemical biosensors, consequently promoting the development of point-of-care systems for applications to personalized therapy.

ACKNOWLEDGMENT

This work was supported by the Swiss National Science Foundation, with the project entitled Intelligent Platform for Drug Response in Precision Oncology, grant number 200021_207900/1.

REFERENCES

- [1] D. Levêque and G. Becker, "The role of therapeutic drug monitoring in the management of safety of anticancer agents: a focus on 3 cytotoxics," *Expert Opinion on Drug Safety*, vol. 18, no. 11, pp. 1009–1015, 2019.
- [2] T. Buclin, Y. Thoma, N. Widmer, P. André, M. Guidi, C. Csajka, and L. A. Decosterd, "The steps to therapeutic drug monitoring: A structured approach illustrated with imatinib," *Frontiers in Pharmacology*, vol. 11, 2020.
- [3] M. Briki, P. André, Y. Thoma, N. Widmer, A. D. Wagner, L. A. Decosterd, T. Buclin, M. Guidi, and S. Carrara, "Precision oncology by point-of-care therapeutic drug monitoring and dosage adjustment of conventional cytotoxic chemotherapies: A perspective," *Pharmaceutics*, vol. 15, no. 4, 2023.
- [4] A. Fuchs, C. Csajka, Y. Thoma, T. Buclin, and N. Widmer, "Benchmarking therapeutic drug monitoring software: a review of available computer tools," *Clinical pharmacokinetics*, vol. 52, pp. 9–22, 2013.
- [5] J. L. Hammond, N. Formisano, P. Estrela, S. Carrara, and J. Tkac, "Electrochemical biosensors and nanobiosensors," *Essays in biochemistry*, vol. 60, no. 1, pp. 69–80, 2016.
- [6] P. Estrela, J. L. Hammond, N. Formisano, P. Estrela, S. Carrara, and J. Tkac, "Electrochemical biosensors and nanobiosensors," *Essays in Biochemistry*, vol. 60, no. 1, pp. 69–80, 06 2016.
- [7] S. Aiassa, S. Carrara, and D. Demarchi, "Optimized sampling rate for voltammetry-based electrochemical sensing in wearable and iot applications," *IEEE Sensors Letters*, vol. 3, no. 6, pp. 1–4, 2019.
- [8] S. Kuroda, S. Kagawa, and T. Fujiwara, "Chapter 12 - selectively replicating oncolytic adenoviruses combined with chemotherapy, radiotherapy, or molecular targeted therapy for treatment of human cancers," in *Gene Therapy of Cancer (Third Edition)*, third edition ed., E. C. Lattime and S. L. Gerson, Eds. Academic Press, pp. 171–183.
- [9] A. A. Khand, S. A. Lakho, A. Tahira, M. Ubaidullah, A. A. Alothman, K. Aljadoo, A. Nafady, and Z. H. Ibupoto, "Facile electrochemical determination of methotrexate (MTX) using glassy carbon electrode-modified with electronically disordered NiO nanostructures," vol. 11, no. 5.
- [10] F. Rodino, M. Bartoli, and S. Carrara, "Simultaneous and selective detection of etoposide and methotrexate with single electrochemical sensors for therapeutic drug monitoring," vol. 7, no. 8, pp. 1–4.
- [11] S. Aiassa, I. Ny Hanitra, G. Sandri, T. Totu, F. Grassi, F. Criscuolo, G. De Micheli, S. Carrara, and D. Demarchi, "Continuous monitoring of propofol in human serum with fouling compensation by support vector classifier," *Biosensors and Bioelectronics*, vol. 171, p. 112666, 2021.
- [12] B.-C. Gu, K.-J. Chung, B.-W. Chen, Y.-H. Dai, and C.-C. Wu, "Electrochemical detection combined with artificial neural networks for the simultaneous intelligent sensing of caffeine and chlorogenic acid," *Electrochimica Acta*, vol. 463, p. 142820, 2023.
- [13] M. Madhiarasan, M. Louzani, *et al.*, "Analysis of artificial neural network: architecture, types, and forecasting applications," *Journal of Electrical and Computer Engineering*, vol. 2022, 2022.
- [14] C. M. Bishop, *Pattern Recognition and Machine Learning*. Springer, 2006.
- [15] A. Mao, M. Mohri, and Y. Zhong, "Cross-entropy loss functions: Theoretical analysis and applications," *arXiv preprint arXiv:2304.07288*, 2023.
- [16] S. Carrara, A. Cavallini, V. Erokhin, and G. D. Micheli, "Multi-panel drugs detection in human serum for personalized therapy," vol. 26, no. 9, pp. 3914–3919.